

Ultraviolet Tomography from CubeSat-based Sensors

Bruce A. Fritz^{*(1)}, Kenneth F. Dymond⁽²⁾, Scott A. Budzien⁽²⁾, and Andrew C. Nicholas⁽²⁾

(1) National Research Council Postdoctoral Research Associate resident at the U.S. Naval Research Laboratory

(2) U.S. Naval Research Laboratory, Washington, DC, 20032

Abstract

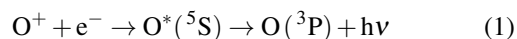
The Triple Tiny Ionospheric Photometer (Tri-TIP) is a compact, ultraviolet (UV) sensor that has been developed as part of the Coordinated Ionospheric Reconstruction Cubesat Experiment (CIRCE). Tri-TIP will measure OI 135.6 nm emissions in the nighttime ionosphere that will be tomographically inverted to determined vertical profiles of electron density in the orbit plane. The Volume Emission Rate Tomography (VERT) method has previously been validated using data from a limb scanning UV spectrometer. The current work will assess the viability of the VERT method when applied to fixed, overlapping view angles from a CubeSat platform.

1 Introduction

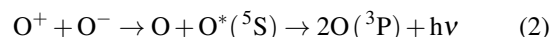
The Triple Tiny Ionospheric Photometer (Tri-TIP) instrument has been developed at the U.S. Naval Research Laboratory as a third generation of remote sensing instruments designed to detect far ultraviolet (FUV) emissions of atomic oxygen in the nighttime ionosphere. [1, 2] Technological advancements have reduced the size of Tri-TIP to a 1U Cubesat form factor (10 cm×10 cm×10 cm). [3, 4] Four Tri-TIP instruments are included on the Coordinated Ionospheric Reconstruction Cubesat Experiment (CIRCE). One of the CIRCE mission objectives is to accurately characterize the dynamic ionosphere by providing tomographic specification of electron density versus altitude derived from simultaneous UV observations of the ionosphere from multiple CubeSats and different view angles. [1]

The Volume Emission Rate Tomography (VERT) approach was developed, in part, to convert Special Sensor Ultraviolet Limb Imager (SSULI) airglow measurements into a two-dimensional map of volumetric emissions in the ionosphere-thermosphere as a function of altitude and orbit phase [5]. Image Space Reconstruction Algorithms (IS-RAs), such as Richardson-Lucy (RL) and Least Squares Positive Definite (LSPD), are based on nonnegative iteration techniques that permit rapid inversion of sparse matrix formulations. The RL and LSPD methods were both demonstrated with simulations and SSULI observations of optically thin OI 91.1 nm nightglow emissions. The inversions were converted to electron density by assuming radiative recombination between oxygen ions and electrons

as the only emission source. [5, 6]



The Tri-TIP optics enable high sensitivity measurements of OI 135.6 nm, as opposed to the optically thin 91.1 nm emission. Recent work has shown the OI 135.6 nm nightglow also depends on mutual neutralization between a positive and negative oxygen ion. [7]



Application of the VERT technique to Tri-TIP measurements requires accounting for both radiative recombination and mutual neutralization, in addition to effects due to radiation transport and radiation transfer. Simulated observations will demonstrate that the CIRCE Tri-TIP instrument configuration will provide sufficient sensitivity and spatial coverage to reconstruct two dimensional plasma density profiles in the nighttime ionosphere.

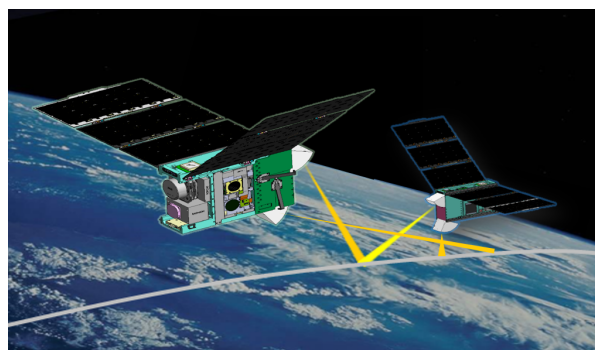


Figure 1. Artist's conception of the CIRCE mission with each Tri-TIP field of view illustrated in yellow.

2 CIRCE Mission

CIRCE is a joint US/UK mission that consists of dual, 6U CubeSats flying in a lead-trail configuration, as illustrated in Figure 1. CIRCE will launch into a circular orbit at $500 \text{ km} \pm 10 \text{ km}$ altitude and $90^\circ \pm 5^\circ$ inclination. Each spacecraft will carry two Tri-TIP instruments with the fields of view oriented to face one another. Both spacecraft will

carry one Tri-TIP pointed along the orbital plane, 45° below the spacecraft velocity vector. The trail spacecraft has a second Tri-TIP oriented along spacecraft nadir, and the lead spacecraft will have a Tri-TIP pointed at the Earth's limb. The limb-viewing Tri-TIP will use a second PMT to extract an additional line of sight along the limb, providing a total of 5 overlapping lines of sight. [1]

The UK contribution to CIRCE is the In-situ and Remote Ionospheric Sensing (IRIS) suite, which consists of three payloads: (i) an ion and neutral mass spectrometer (INMS), (ii) a radiation monitoring package (RadMon), and (iii) a GPS receiver (TOPCAT) that uses signal propagation delay to map the ionosphere. The IRIS suite fits within a 2U CubeSat volume and will occupy the opposite side of the spacecraft as Tri-TIP. [1]

The Tri-TIP detectors provide order of magnitude higher sensitivity than typical UV spectrometers. [2] Tomographic reconstructions using limb-scanning UV spectrometer measurements have been used to provide vertical profiles of physical parameters, such as electron density in the ionosphere. [5, 6] This work explores whether the algorithms used to invert limb-scanning measurements will provide similar results with fixed lines of sight from a CubeSat platform. This will help determine the degree to which CIRCE will satisfy its objective of characterizing the two-dimensional distribution of electrons in the orbital plane of the spacecraft.

3 Tomographic methodology

The Volume Emission Rate Tomography (VERT) method converts measurements of airglow brightness, $4\pi I$, in units of Rayleighs (10^6 photons/s/cm² emitted into 4π steradians), into a two dimensional map of ϵ , or volume emission rate (VER), in units of photons/s/cm³, by inverting the equation for brightness along a line of sight.

$$4\pi I = 10^{-6} \int_0^{\infty} \epsilon(z, \lambda, \phi) ds(z, \lambda, \phi) \quad (3)$$

The brightness is calculated as a function of altitude (z), latitude (λ), and longitude (ϕ) and then integrated over the line of sight distance (s). The integral is normally inverted by discretizing into voxels where VER is assumed constant. In the current work, however, the VER is assumed to vary bicubically and the integrals are discretized with bicubic spline weighting, W_i , and quadrature weight, G_i .

$$I_{1356} = 10^{-6} \sum W_i G_i \epsilon(z_i, \phi_i) T(\delta\tau, \delta t) \Delta s_i \quad (4)$$

The Holstein transmission function, $T(\delta\tau, \delta t)$, also accounts for photon scattering ($\delta\tau = |\tau(s_i) - \tau(0)|$) and photon absorption ($\delta t = |t(s_i) - t(0)|$) between the source and

observer. The ‘‘T’’ function integrates over all photon frequencies to model the radiation transfer along the path length, s_i , from observer to the i th point on the line of sight. The volume emission rate in this equation has already undergone radiation transport, whereby photons are redistributed from the initial output ($\epsilon_0 \rightarrow \epsilon$) using the integral version of radiation transport equation in the plane-parallel Complete Frequency Redistribution approximation. [8]

An optically thin emission like OI 91.1 nm can be inverted by assuming only radiative recombination drives the emission rate, $\epsilon_0(z, \lambda, \phi) = \alpha n_e(z, \lambda, \phi) n_{O^+}(z, \lambda, \phi)$. The electron density, n_e and oxygen ion density, n_{O^+} , are related by the radiative recombination rate coefficient, α , to produce photons at the given rate, ϵ_0 . In the peak F region, quasi-neutrality assumes that $n_e \approx n_{O^+}$, which simplifies the nightglow emission source to $\epsilon_0 = \alpha n_e^2$. OI 135.6 nm emissions, on the other hand, require additional terms to account for the mutual neutralization reaction. [7]

$$\epsilon_0(z) = \gamma \beta_{1356} \frac{k_1 k_2 n_e n_{O^+}(z)}{k_2 n_{O^+} + k_3 n_{O^+}(z)} + \gamma \alpha_{1356} n_e(z) n_{O^+}(z) \quad (5)$$

Reaction rate coefficients (k_1, k_2, k_3), the radiative recombination rate coefficient (ϵ_{1356}), the production fraction (β_{1356}), and the branching ratio (γ) are all constants determined in a laboratory.

The VERT approach solves Equation 4 for the volume emission rate based on measurements of airglow brightness, I_{1356} . A matrix of observations is inverted into a grid of, ϵ , as a function of altitude and orbit phase. Once photons are created and distributed via radiation transport, the CFR method is used to calculate the radiation transfer and the effects are corrected in the VER grid. Finally, Equation 5 is inverted to derive the electron density. Atomic oxygen density (n_O) is derived from the NRLMSISE-00 model, and in the nighttime F region the $n_{O^+} \approx n_e$ assumption is still applied. Figure 2 illustrates a validation of the VERT technique using SSULI measurements of OI 135.6 nm. [7]

The top panel in Figure 2 shows electron density measurements made by the Advanced Research Project Agency Long-range Tracking and Identification Radar (ALTAIR) incoherent scatter radar (ISR) on 26 August 2010. The middle panel illustrates the results of inverting SSULI measurements without accounting for the mutual neutralization photochemical reaction, or the effects of radiation transfer/transport. The bottom panel adds in the missing physics and chemistry to create a more physically realistic result. In this example, the middle panel results in a mean error of 19% between the ALTAIR and SSULI measurements and the bottom panel improves the result to a 13% mean error with radiation transport, transfer, and mutual neutralization included.

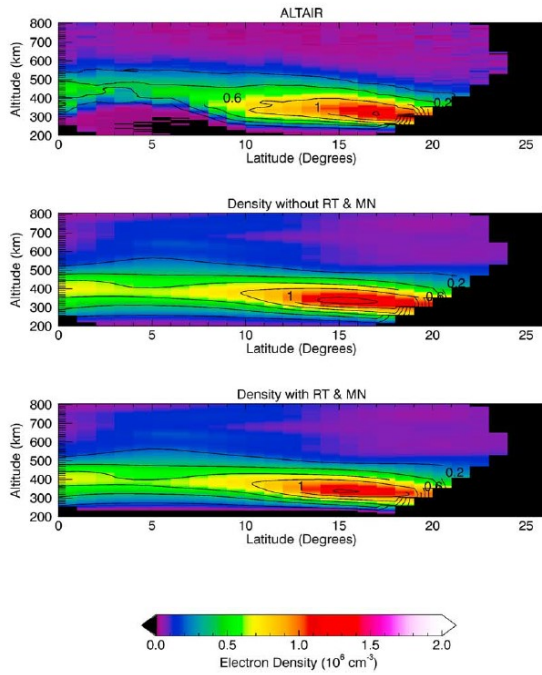


Figure 2. (Top) ALTAIR ISR measurements of electron density at low latitudes; (Middle) Sample VERT reconstruction using SSULI measurements of OI 135.6 nm at low latitudes assuming only mutual neutralization; (Bottom) VERT reconstruction using full physics and chemistry (see text for details). [7]

4 Tomography simulations

Observations by CubeSat remote sensors at fixed observing angles may be simulated with a model atmosphere to demonstrate the feasibility of performing tomographic reconstructions. A model atmosphere is established with the NRLMSISE-00 and International Reference Ionosphere (IRI) empirical models to generate maps of neutral and electron density in the thermosphere and ionosphere, respectively. The empirical values of n_e , n_{O^-} , and n_{O^+} are fed into Equation 5 to produce a map of volume emission rate, ϵ_0 , as a function of altitude along the orbit plane. The photons “created” using the appropriate photochemical reaction are then redistributed using the CFR radiation transport method, converting the original emission rate ϵ_0 into the physically realistic rate, ϵ .

The next step in the simulation is to “fly” spacecraft through the region to simulate what the Tri-TIPs would see given the expected mission parameters, including the specific instrument look angles and sensitivity. The brightness “observed” by the spacecraft, I_{1356} , is calculated by inserting the volume emission rate, ϵ , into Equation 4. Radiation transfer is included as part of the observation scenario, and realistic noise is superimposed on the simulated measurements. Finally, tomographic inversions are performed on the simulated set of observations to determine if the initial volume emission rate can be reproduced. The VERT maps

are then inverted into other physical quantities like electron density to compare with the empirical quantities used to initiate the simulations.

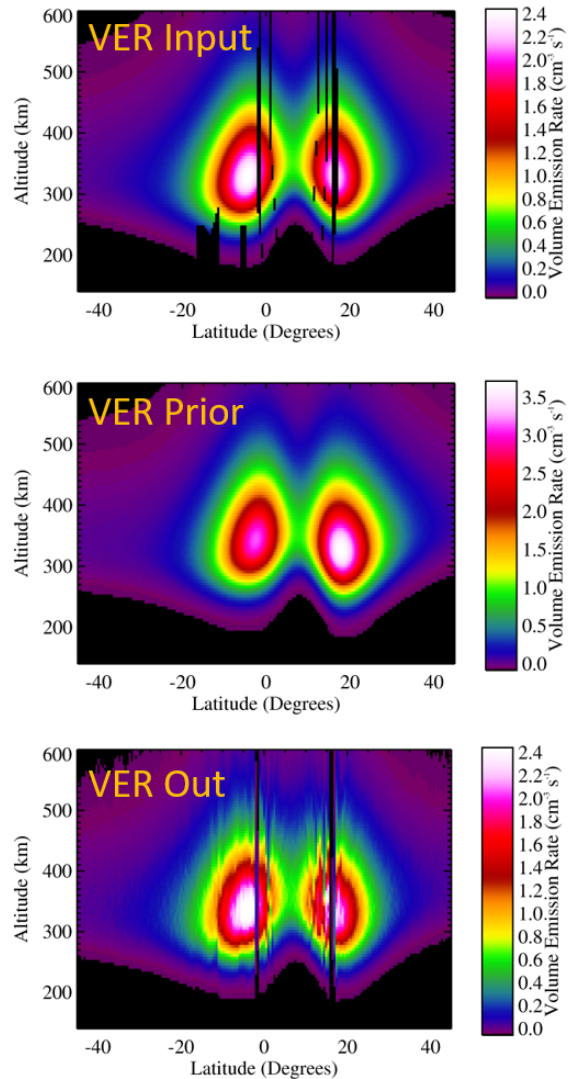


Figure 3. Simulated reconstruction using CIRCE viewing geometry. Ionospheric parameters are derived from IRI-2007. (Top) Input ionosphere is 3:30 local time, 52° E longitude. (Middle) Prior ionosphere is prior ionosphere calculated at 2:15 local time, 34° E longitude, then multiplied by a factor of $\times 3$ (Bottom) Tomographic reconstruction of the input using the prior “guess at the solution.”

Standard reconstructions of the ionosphere have shown very good agreement between the input VERT and the retrieved map of density. Figure 3 shows the results of simulations using the CIRCE viewing geometry. This simulation uses an input ionosphere at 3:30 local time (LT), 52° E longitude and a prior ionosphere at 2:15 LT, 34° E longitude. Maps of quiet conditions have shown remarkable consistency between the input and retrieved output (IRI-2007 ionosphere, midnight, 0° longitude, 10.7 cm flux = 200 SFU). The algorithms require a “guess” at the initial state and tests have shown that a uniform background

($1 \times 10^{-3} \text{cm}^{-3} \text{s}^{-1}$) is not sufficient to reproduce structure like seen in the Equatorial Ionization Anomaly (EIA). However, a guess using the IRI several hours apart and times a factor 3 in density, which is shown in the middle panel of Figure 3, shows that the expected initial rate can be retrieved with a high level of agreement.

More challenging scenarios add ionospheric disturbances to the input, such as bubbles. The LSPD retrieval works well, as the vertical bubble structures are reproduced and overall structure is in agreement with the input (agreement better than 10%). The bottomside bubbles, however, are not reproduced, and their emission rates are larger than the input.

5 Summary

Simulated tomographic reconstructions using the VERT method show that a dual CubeSat mission like CIRCE is capable of imaging plasma density structures in the nighttime ionosphere. Five fixed lines of sight are sufficient to produce the large scale structure in the ionosphere, such as the EIA. Smaller scale structures like bubbles and scintillation are more challenging and may depend on coincident observations, like profiles from GPS RO or in situ measurements of ion and neutral species. The impact of adding GPS radio occultation profiles or in situ measurements to the CIRCE Tri-TIP retrievals may be analyzed in the future to evaluate the total mission potential.

6 Acknowledgements

Bruce Fritz is an NRC Postdoctoral Research Associate at the U.S. Naval Research Laboratory. All authors are supported by the Chief of Naval Research.

References

- [1] A. C. Nicholas, G. D. R. Attrill, K. F. Dymond, S. A. Budzien, A. W. Stephan, B. A. Fritz, G. J. Routledge, J. A. Miah, C. M. Brown, P. J. Marquis, T. T. Finne, C. N. Mitchell, R. J. Watson, D. O. Kataria, and J. Williams, "Coordinated Ionospheric Reconstruction CubeSat Experiment (CIRCE) mission overview," *CubeSats and SmallSats for Remote Sensing III*, **11131**, International Society for Optics and Photonics, SPIE, 2019, pp. 105–117, doi: 10.1117/12.2528767.
- [2] S. Budzien, B. Fritz, A. Stephan, P. Marquis, S. Powell, B. O'Hanlon, A. Nicholas, K. Dymond, and C. Brown, "Comparison of second and third generation 135.6 nm ionospheric photometers using on-orbit and laboratory results," *CubeSats and SmallSats for Remote Sensing III*, **11131**, International Society for Optics and Photonics, SPIE, 2019, pp. 1–13, doi: 10.1117/12.2528791
- [3] B. A. Fritz, A. W. Stephan, P. W. Walker, C. M. Brown, A. C. Nicholas, K. F. Dymond, S. A. Budzien, P. J. Marquis, T. T. Finne, and K. D. Wolfram, "Ultraviolet beam splitter characterization for use in a CubeSat optical system," *Journal of Applied Remote Sensing*, **13**, 3, pp. 1–11, 2019, doi: 10.1117/1.JRS.13.032503.
- [4] A. W. Stephan, P. J. Marquis, S. A. Budzien, K. F. Dymond, C. M. Brown, K. D. Wolfram, and A. C. Nicholas, "Evaluation of UV optics for triple tiny ionospheric photometers on CubeSat missions," *Proc. SPIE, CubeSats and NanoSats for Remote Sensing II*, **10769**, 2018, doi: 10.1117/12.2321042.
- [5] K. F. Dymond, S. A. Budzien, and M. A. Hei, "Ionospheric-thermospheric UV tomography: 1. Image space reconstruction algorithms" *Radio Science*, **52**, 3 February 2017, pp. 338–356, doi: 10.1002/2015RS005869.
- [6] K. F. Dymond, A. C. Nicholas, S. A. Budzien, A. W. Stephan, C. Coker, M. A. Hei, and K. M. Groves, "Ionospheric-thermospheric UV tomography: 2. Comparison with incoherent scatter radar measurements," *Radio Science*, **52**, 3, February 2017, pp. 357–366, doi: 10.1002/2015RS005873.
- [7] K. F. Dymond, A. C. Nicholas, S. A. Budzien, A. W. Stephan, C. Coker, M. A. Hei, and K. M. Groves, "A Comparison of Electron Densities Derived by Tomographic Inversion of the 135.6-nm Ionospheric Nightglow Emission to Incoherent Scatter Radar Measurements," *Journal of Geophysical Research: Space Physics*, **124**, May 2019, doi: 10.1029/2018JA026412.
- [8] R. R. Meier, "Ultraviolet spectroscopy and remote sensing of the upper atmosphere," *Space Science Reviews*, **58**, 1, 1991, pp. 1–185, doi: 10.1007/BF01206000.